CHAPTER 17

Subcooled Boiling

F. Mayinger

1 INTRODUCTION

The practical layout of heat exchangers and steam generators, especially in earlier times, was based only on the assumption that boiling does not start before the mean temperature in the liquid has reached its saturation point; that is, the beginning of the first bubble formation was calculated by an energy balance according to the first law of thermodynamics. This assumption is not valid at high heat-flux densities as they exist, for example, in oil-fired boilers, in heat exchangers with great temperature differences between the primary and the secondary fluid, and especially in the core of water-cooled nuclear reactors.

At high heat-flux densities, vaporization may occur at the heated surface despite the fact that the mean temperature of the cooling liquid has not yet reached the saturation point. This phenomenon is called "subcooled boiling," which is caused by a thermodynamic nonequilibrium in the liquid. There is a superheating of the liquid in the boundary layer near the heated wall, while the bulk temperature is still fairly subcooled. Bubbles formed near the wall grow at first because of heat and mass transfer from the superheated boundary layer, but then, by further enlarging their volume or by movement, they move beyond the superheated boundary layer and start to condense again where, by now, the heat transfer is reversed.

Regarding a cooling channel with high heat-addition where subcooled liquid enters, in the literature four zones are usually distinguished, as shown in Fig. 1.

In zone I, because of the high subcooling of the liquid, there is pure single-phase flow. The heat transfer from the wall to the fluid takes place by forced convection only. Because of heat addition, the temperature of the cooling liquid rises and, eventually, the wall temperature reaches a point at which bubble formation starts on technical rough surfaces; that is, the boiling nuclei become active but the subcooling of the fluid is still high

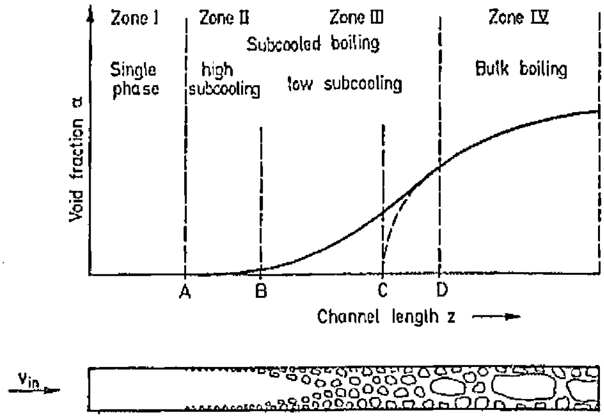

FIG. 1 Boiling regions in subcooled flow boiling.

enough that the bubbles cannot grow far beyond the very thin superheated boundary layer, and they are recondensed immediately as soon as their top enters the subcooled zone. Looking at this phenomenon, one gets the impression that the bubbles adhere to the wall. In zone II, the steam content of the void is very low and is regarded as a pure wall effect.

Flowing along the channel, the difference between saturation temperature and bulk temperature of the fluid becomes smaller. The bubbles formed in the superheated boundary layer can now detach from the heated surface and slowly condense downstream in the subcooled bulk. From this point of the bubble detachment (marked B in Fig. 1), the void in zone III increases rapidly. The fluid is not in thermodynamic equilibrium because in the subcooled bulk there are a lot of vapor bubbles also having a short duration of life. Further downstream, the fluid finally reaches thermodynamic equilibrium and then we have pure net steam production.

This phenomenon of subcooled boiling for the present represents a compensating safety potential if the layout of the heat exchanger is insufficient, because the heat-transfer conditions are improved when boiling starts and, thus, local temperature differences are diminished. The bubble formation due to subcooled boiling, however, can result in very severe disturbances of the flow even in a breakdown, because of the well known fact that the two-phase flow has a much higher pressure drop than the single-phase one. Often ignored or not sufficiently considered regarding these boiling phenomena, there is the danger that, for example, the layout of the pump for a loop is inadequate or that flow instabilities may occur, i.e., periodic changes in the mass flow rate.

For predicting the beginning of boiling and the real quality or void in heat exchangers and steam generators with high heat-flux densities, there are several theoretical models, all of which involve many empirical assumptions. For the present, we mention just the models and theoretical treatments of Bowring

(1962), Levy (1966), Lavigne (1962), Tong (1967), and Rouhani (1968). The uncertainty of these theoretical models results mainly from

1 Empirical assumptions regarding the beginning of boiling; that is, the first bubble formation
2 The mathematical description of bubble formation and bubble growth
3 The physically correct description of bubble condensation

All these processes are a function of the temperature decay in the boundary layer near the wall and at the phase boundary between the bubbles and the liquid. For a better understanding, it therefore seems suitable to discuss the peculiarities of bubble formation in subcooled liquids first.

2 BUBBLE FORMATION AND BUBBLE COLLAPSE IN SUBCOOLED LIQUIDS

As is well known, there is a greater number of publications describing the boiling phenomena in saturated liquids and, today, there is general understanding and agreement that bubbles start from roughnesses; that is, small cavities in the heated wall. The heat stored as latent heat in the vapor of the bubble is attained there on a detour from the superheated liquid boundary. But the bubble does not carry latent heat only in the vapor; in addition, because of the high turbulence caused by detaching from the wall, it transports heat in the liquid drift flow behind it. Regarding the heat and mass transfer between the superheated boundary layer and the forming vapor bubble, there are a lot of theoretical and experimental works that cover a wide field of assumptions, starting from pure heat conduction in the liquid boundary up to high convective eddies produced by differences in surface tension over the bubble circumference. One may mention, for example, the papers by Forster and Zuber (1955), Han and Griffith (1965), Plesset and Zwick (1954), Beer (1969), and Winter (1971). Reliable statements about the real behavior require measuring techniques of the highest accuracy. The conventional measuring devices very often are too slow or even influence the process to a nonpermissible extent. Endeavoring to get more information about the subcooled boiling phenomena we used, besides the well known microthermocouples, a new optical method, the so-called holographic interferometry, in our laboratory at the Technical University, Hannover. It would take too much space to describe this measuring technique in detail; therefore, only a few results worked out by this method and with the help of high-speed cinematography will be pointed out here.

In spite of long years of research work in bubble boiling, even under saturated conditions, as Fig. 2 shows, there are very different statements about bubble formation, especially bubble growth.

Recent calculations as, for example, by Beer (1969), who takes into

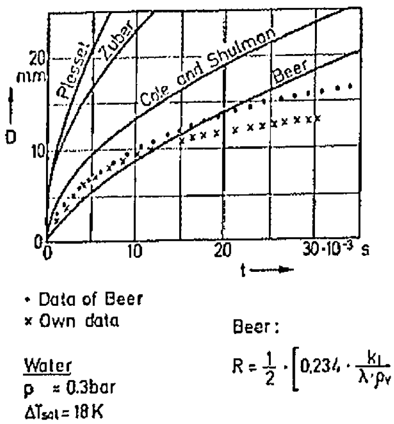

Plesset and Zwick:

$$R = \sqrt{3} \cdot \frac{2 \cdot k_l \cdot \Delta T_{sat}}{\lambda \cdot \rho_v \cdot \sqrt{\pi \cdot a_l}} \cdot \sqrt{t}$$

Forster and Zuber:

$$R = \frac{\pi}{2} \cdot \frac{2 \cdot k_l \cdot \Delta T_{sat}}{\lambda \cdot \rho_v \cdot \sqrt{\pi \cdot a_l}} \cdot \sqrt{t}$$

Cole and Shulman:

$$R = \frac{\pi}{4} \cdot \frac{2 \cdot k_l \cdot \Delta T_{sat}}{\lambda \cdot \rho_v \cdot \sqrt{\pi \cdot a_l}} \cdot \sqrt{t}$$

Beer:

$$R = \frac{1}{2} \cdot \left[0.234 \cdot \frac{k_l}{\lambda \cdot \rho_v} \cdot \left(\frac{\rho_l \cdot \Delta a}{\mu_l^2 \cdot \Delta \varphi}\right)^{0.55} \cdot Pr^{1/3}\right]^{0.69} \cdot \Delta T_{sat}^{0.69} \cdot t^{0.59}$$

FIG. 2 Bubble growth in saturated pool boiling.

account the so-called Marangoni effect, influencing the heat and mass transfer at the phase boundary, seem to give better results. Whereas the bubble at saturated conditions reaches its equilibrium asymptotically, in subcooled boiling the condensation process starts very early, sometimes even superimposing on the growing behavior. Because of this, the prediction of bubble formation and bubble collapse is very difficult.

As can be seen from holographic pictures taken with a high-speed camera, the superheated boundary layer at the heated wall is formed relatively slowly at the beginning, and suddenly a bubble grows out of it which then, depending on the liquid temperature outside the superheated boundary layer, condenses again. The condensation process starts primarily at the top of the bubble. This causes a very violent circulation around the bubble to be produced and then the heat exchange prevails at the lower parts of the bubble because of liquid eddies formed by the bubble movement. One can also see partially during the condensation a compression and extension process, which may result in a superheating or subcooling of the vapor in the bubble. This results in a pulsating and very unstable bubble collapse.

The growing of a bubble takes about one-tenth the time needed for the succeeding condensation. In principle, one can use equations for the condensation similar to those for bubble growth, and several formulations are given in the literature, which differ mainly in treating the heat transfer at the phase boundary and in considering the inertia effects. They all assume the spherical shape of the bubble and uniform conditions over the bubble circumference. In Fig. 3, the calculated results of some mostly new theories are presented and compared with measured results.

As can be seen, there is not the best agreement. The dynamic behavior of the condensation can be best seen if one calculates the first and second derivatives from the growing and collapsing curves. One then gets the growing and collapsing velocities and also the acceleration. This was done in Fig. 4 for

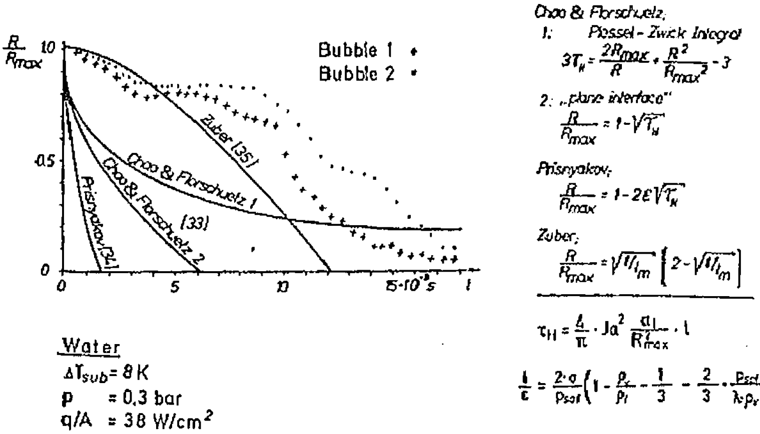

FIG. 3 Bubble condensation in subcooled pool boiling: theoretical and experimental results.

he example mentioned above. The bubble growth and collapse was measured n this example, as shown by a high-speed camera, and one can see from the neasuring points that there seems to be an oscillating behavior of the bubble rolume during condensation. Because of the two-dimensional photographic echnique, we are not sure whether this is a real oscillation or whether, recause of the rotating movement of the not real spherical bubble, there is

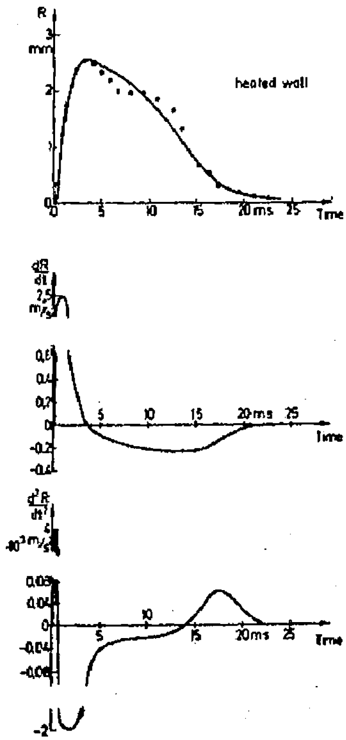

FIG. 4 Bubble growth and condensation in subcooled pool boiling with first and second derivatives

only the impression of an oscillation. Therefore, in calculating the velocity and the acceleration, we took smoothed values. Figure 4 shows that the growing velocity can be as large as 2.5 m/s and that the velocity of the phase boundary during condensation reaches values of −0.2 m/s. From this, one can derive a very high acceleration that changes in sign several times. The acceleration in this example was measured with 4.10^3 m/s^2 as maximal value.

All these highly dynamic motions have to be taken into account working out a theoretical model for predicting bubble growth and collapse, and, therefore, one cannot limit the deliberations to the heat and mass transfer at the phase boundary. Because of the high phase velocities, one usually cannot assume thermodynamic equilibrium between vapor and liquid. Also, a model based only on inertia effects does not conform to reality. An answer to the temperature conditions in the boundary and around the bubble is given by holographic interferometry. But just these measurements show, as can be seen from the next two figures, that the temperature distribution is formed by a process very statistical in nature. Figure 5 shows the temperature around a so-called "primary bubble." The black lines represent isotherms in a first approximation, and one can see that there is a great temperature gradient at the bottom, or root, of the bubble. At its top, the bubble is covered with a thin liquid layer of saturation temperature. From this, it is evident that there is a great difference of surface tension forces around the bubble, which may result in eddy circulation, improving the heat transfer process. To give an idea of the dimensions, it should be mentioned that the heater (seen as a black line) was 0.4 mm thick and that the bubble had a diameter of a few millimeters. Above the top of the bubble there seems to be a uniform undisturbed temperature. This is not always the case, and in Fig. 6 one can see quite different conditions in the phase boundary around the bubble. Here,

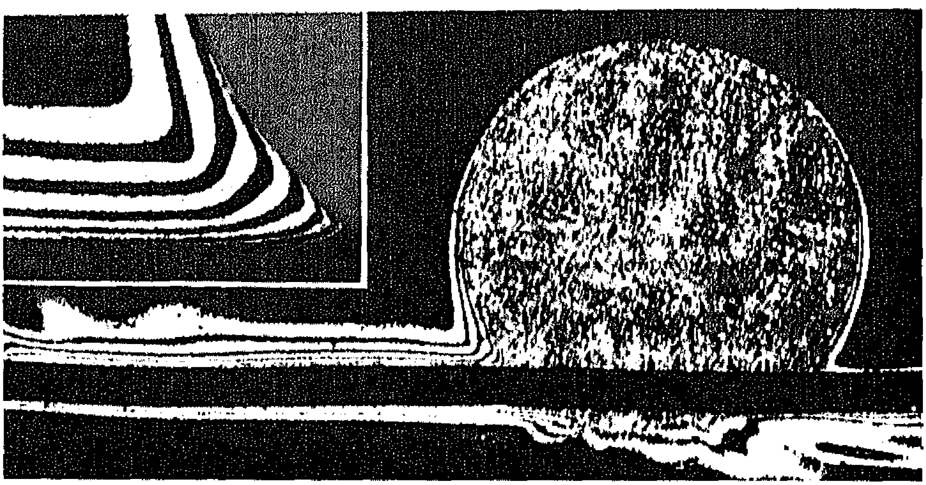

FIG. 5 Temperature distribution around a growing "primary bubble." Water, $p = 0.4$ bar, $\dot{q} = 46$ W/cm^2, subcooling = 3K.

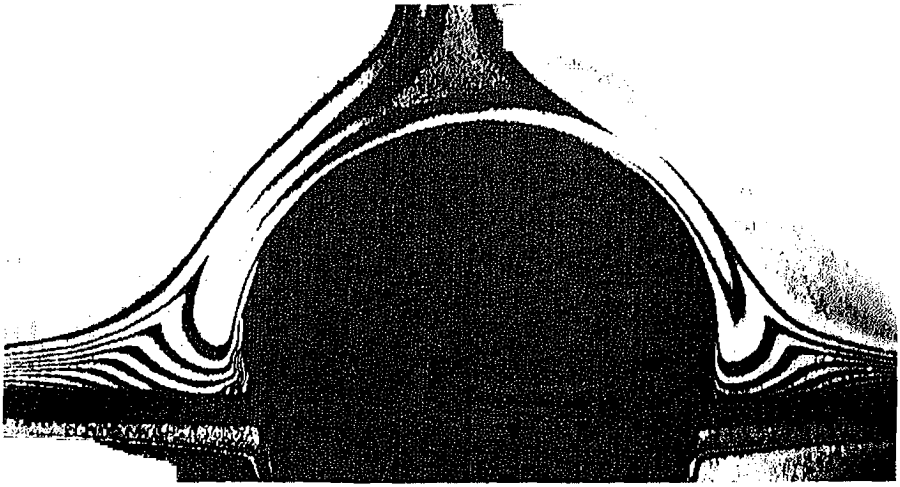

FIG. 6 Temperature distribution around a "secondary bubble." Water, $p = 0.3$ bar, $\dot{q} = 30\ W/cm^2$, subcooling = 2K.

because of the drift flow of the preceding bubble, there still is a very clearly developed temperature field. The bubble growing beneath this field we call a "secondary bubble." One can easily imagine that the growing and condensing conditions for this bubble are quite different from the one discussed before.

The bubbles shown in the last two figures were still in the growing period. The beginning of the condensation is shown in Fig. 7. At the top of the

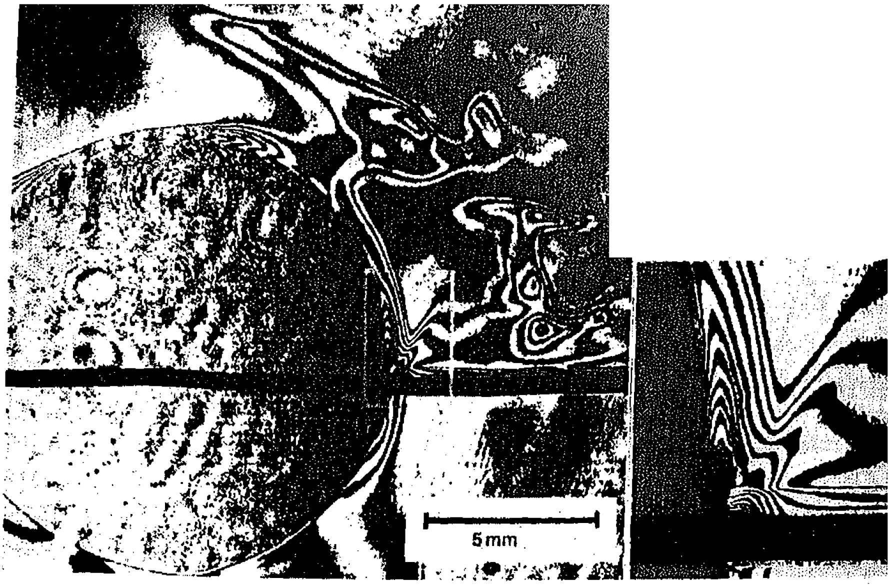

FIG. 7 Temperature distribution around a growing "primary bubble"; condensation at the top of the bubble. Water, $p = 0.4$ bar, $\dot{q} = 46\ W/cm^2$, subcooling = 3K.

bubble and at its right side, condensation starts from the narrowly spaced and sharply bending fringes in the phase boundary. The starting point of the recondensation usually is to be found at the top of the bubble, but, statistically, there also may be, in addition, a first recondensation at any portion of the upper part of the bubble. If we were to follow the condensation process further, we would see that, after the beginning of the condensation at the top of the bubble, a very violent circulation starts around the bubble, which transports cold liquid to the bubble root and now initiates further condensation at the bubble foot, while the top is covered with a thin layer of saturated liquid insulating the vapor from the subcooled fluid. This insulating layer is stabilized during the bubble detachment, so one could calculate the heat transfer process between vapor and liquid according to the flow conditions around a sphere with a maximum of heat transport in the eddies of the drift flow. But, in addition, there are inertia effects.

Further information for elaborating theoretical models could be taken from the temperature profile in the liquid near the wall, as shown in Fig. 8. With the wall distance as the abscissa, the measured minimum and maximum temperatures are plotted. In addition, there is shown the temporal mean value of the local boundary temperature. The local temperature in the boundary is subject to very strong high-frequency changes, as also shown in the figure. The

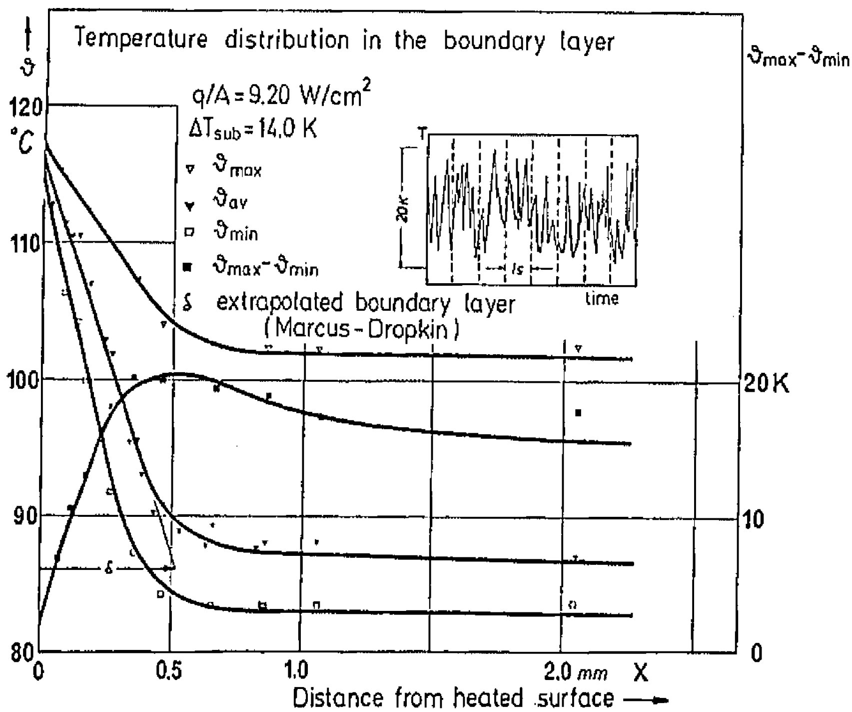

FIG. 8 Temperature profiles in the boundary layer over a heated horizontal copper plate.

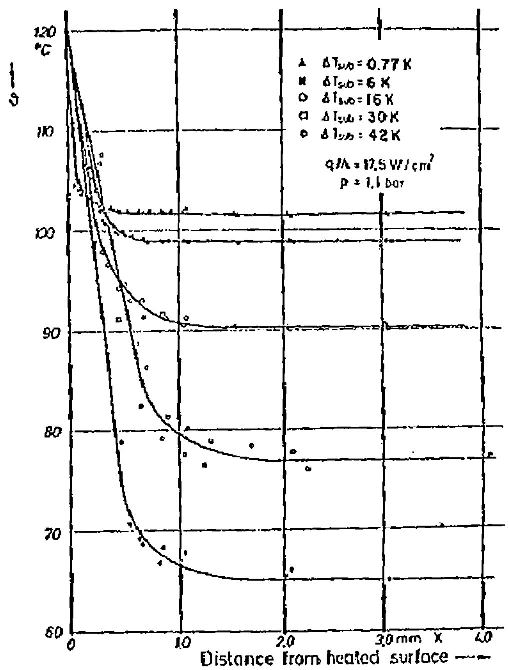

FIG. 9 Time-averaged temperature profiles over a heated copper plate with various subcoolings.

mean temperature was calculated by integrating this oscillating curve. In the immediate neighborhood of the heated wall, the amplitudes of the temperature changes are naturally determined by the heat capacity of the wall material. In this example, the heated wall was made of a thick piece of copper having high heat capacity and good heat conductivity. The distance at which the temperature oscillations reach their maximum value depends on the subcooling of the liquid and on the heat flux density. With diminishing subcooling, it approaches the wall. Under the conditions of subcooled boiling, the maximum of these oscillations is to be expected in such a distance where the condensation starts. This is usually in a distance of 0.2–0.5 mm. The temperature curve in the boundary layer, as the figure shows, is linear at the beginning and then approaches asymptotically in an *e*-function to the bulk temperature of the fluid.

From the literature, it is known that, with saturation boiling, the gradient of the temperature distribution in the boundary layer becomes greater with growing heat-flux density, which can perhaps be explained in a simple manner by the fact that, in the very first time till the bubble is formed, the heat transport has to be managed by pure conduction in the fluid. For calculation with subcooled boiling, one also has to know the dependency of this temperature distribution on the subcooling. Figure 9 shows the time-averaged curves of the fluid temperature for different subcooling at constant heat-flux density. One can see that the temperature gradient in the immediate vicinity of the wall is low, or only a weak function of the bulk temperature, that is, of the subcooling.

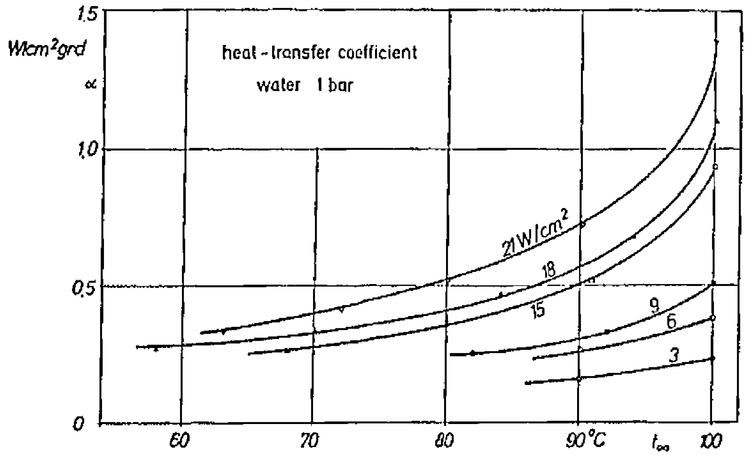

FIG. 10 Heat-transfer coefficients with subcooled boiling at free convection. Water, $p = 1$ bar.

From these measurements, one can derive heat-transfer coefficients, as done in Fig. 10, for low-pressure free-convection subcooled boiling. The heat-transfer behavior shown there reaches from values measured at low heat-flux densities, which fully correspond to pure free-convection conditions, to the high values of fully developed saturation boiling.

3 MEASUREMENTS OF BUBBLE FORMATION AT FORCED CONVECTION

The measurements presented up to now were all taken with free convection and low pressures. From additional measurements under forced convection, we got the impression that the conditions for the bubble formation in the boundary layer near to the wall do not change appreciably. This may be caused by the fact that the bubbles at the wall break down the flow velocity so much that the axial convection has little or no influence on the bubble formation. This is well known for the behavior of the heat-transfer coefficient with boiling. There is, up to a certain quality, almost no influence of flow velocity. But the mass flow rate influences the bulk temperature via the energy balance, and thus the subcooling of the liquid. In a technical heat exchanger, in addition, the complicated geometric conditions, for example, the arrangement of the rods in a cluster, have an influence on the first bubble formation as well as on bubble growth and collapse.

A very important question for calculating subcooled boiling is the determination of the location where, under forced conditions in a channel, the first bubble formation starts. Measurements done at high pressure and at flow rates in the technically interesting range showed that the beginning of bubble formation is also strongly dependent on the shape of the cross-section of the channel. In Fig. 11, experimental results are presented that were gained in a four-rod bundle. The rods of this bundle were uniformly heated. It is easy to

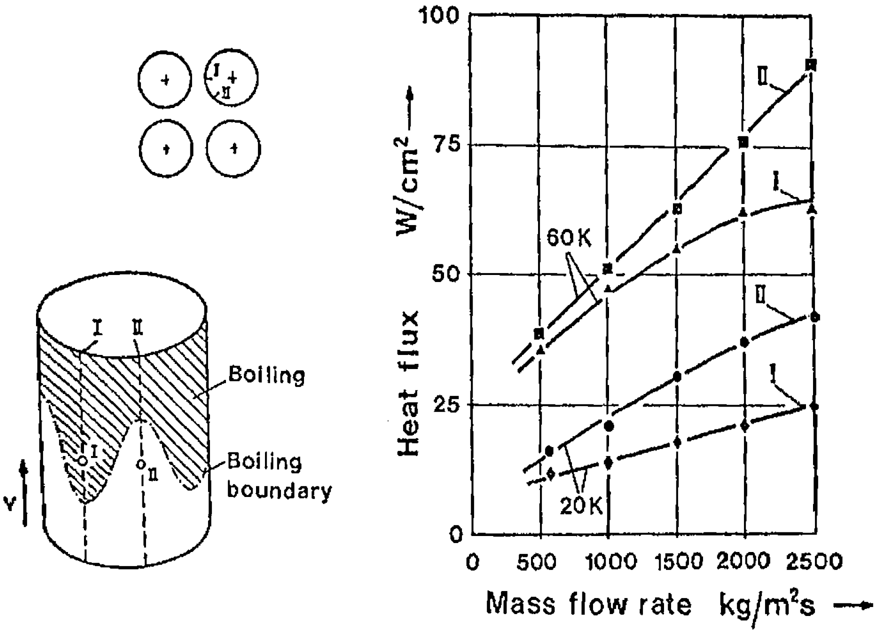

FIG. 11 Beginning of bubble formation in a four-rod bundle at forced convection subcooled boiling.

imagine that, in the most narrow gap between two rods, there is a smaller mean velocity than in the diagonal position. Therefore, boiling starts first in the narrow gap, and the boundary line for incipient boiling, as shown in the figure, has a cosine form around the circumference of each rod. The heat-flux conditions under which subcooled boiling at these circumferential rod positions starts may differ very strongly, as shown in the right part of the figure.

In Fig. 12, for a pressure of 100 bar and for different mass flow rate

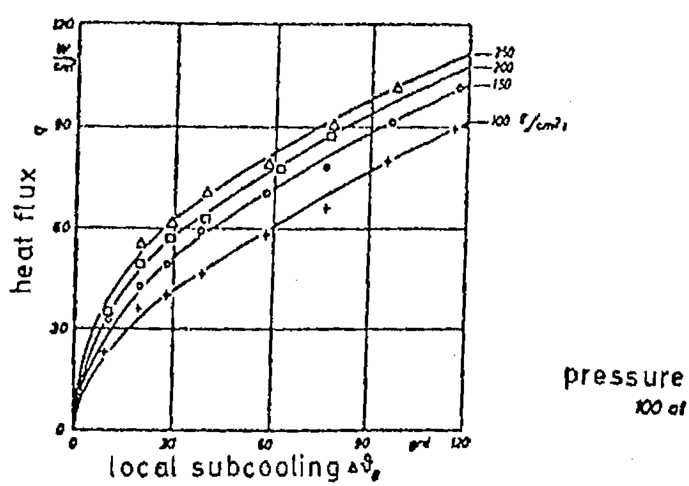

FIG. 12 Beginning of subcooled flow boiling in a four-rod bundle.

densities, the beginning of subcooled boiling is plotted. One can see that, at low subcooling, boiling already starts at very small heat-flux densities, and even at high subcooling, the heat-flux conditions for incipient boiling lay well within the range sometimes existing in oil- or gas-fired boilers, but always present in pressurized water reactors. But these basic considerations of the physical process would not be complete if we did not mention in this connection, another very important factor in the typical behavior of two-phase flow before treating theoretical models for calculating void fraction in subcooled boiling. Thus, in addition, we have to consider the slip ratio which, as pointed out already in detail in this course, is a function of different hydrodynamic and thermodynamic parameters, such as mass flow rate, pressure, and quality.

4 THEORETICAL MODELS

For calculating the void fraction in subcooled boiling, we have to know

1 The location or the subcooled temperature in the channel where the first bubbles are formed at the heated wall
2 The subcooled temperature or the location in the channel where the vapor bubbles detach from the wall
3 The heat and energy distribution in the fluid, i.e., the amount of heat that got into the liquid and into the vapor, respectively; one has to keep in mind that there is thermodynamic nonequilibrium, i.e., the mean specific enthalpy of the fluid is smaller than the enthalpy of the saturated liquid
4 The recondensation rate of the detached bubbles in the channel from the point where they departed from the wall up to the location where saturated boiling is reached
5 The slip ratio

From the several theoretical models (Bowring, 1962; Levy, 1966; Lavigne, 1962; Rouhani, 1968) for predicting void fraction in subcooled boiling, we shall discuss the basic ideas of Bowring (1962) and then we shall treat the model of Rouhani (1968) in more detail.

4.1 Bowring's Model

In Fig. 1 we discussed qualitatively the amount of void fraction at subcooled boiling. Figure 13 shows a more detailed sketch of the heat-transfer domains in a heated channel.

Bowring assumes that the first area (AB in Fig. 13) makes almost no contribution to the steam voidage in the channel, and that a rapid increase in void fraction starts from point B in Fig. 13, which represents the condition needed for bubbles to leave the surface. It is this second region, BCD, that is the main subject of his theory.

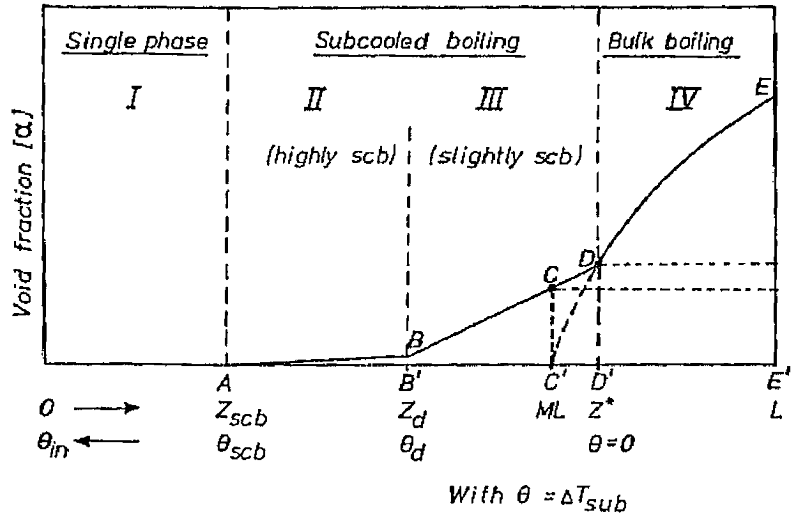

FIG. 13 Sketch of the heat-transfer domains in a heated channel.

For a long heated channel with heat-transfer regions, as shown in Fig. 13, the transition subcooling, θ_r, at which the void fraction begins to rise rapidly is that at which the bubble detachment occurs. This is not, however, a unique criterion for θ_r, as the subcooling at which boiling starts, θ_{scb}, may be lower than the temperature difference at which the bubbles detach, θ_d. A third possibility is that the channel inlet subcooling may be less than both above-mentioned temperatures, that is, less than θ_{scb} and less than the detachment subcooling θ_d.

We now need a condition for subcooled boiling to start which is simply defined by Bowring as that condition when the heated surface temperature reaches saturation temperature plus the degree of superheat, given by an equation for nucleate boiling heat transfer, for example, by the equation of Jens and Lottes (1951):

$$t_w - t_s = \beta\left(\frac{q}{A}\right)^{0.25} \tag{1}$$

By doing so, we get for the temperature at which boiling starts

$$\theta_{scb} = \frac{q}{Ah} - \beta\left(\frac{q}{A}\right)^{0.25} \tag{2}$$

In this equation, β has the value 7.8 exp $[-0.0163(p-1)]$. The units used in this equation are K, W, m, and atm, respectively. As done by Bowring, one also can evaluate the subcooling at which detachment occurs in a purely empirical way with the help of an empirical parameter. From measurements, Bowring assumes that the temperature at which detachment occurs is a function of velocity, heat-flux, and pressure, but not of geometry. As shown in Chap. 3, this is true only if the local velocity is known. Bowring correlates the temperature at which the bubbles detach by the simple equation

$$\theta_d = \frac{\eta q}{A v} \tag{3}$$

in which η is a so-called subcooled void parameter, depending only on the pressure of the liquid. For water, Bowring gives the relation

$$\eta = \frac{v\theta_d}{q/A} = 14 + 0.1p \tag{4}$$

This equation is valid in the range between 11 and 136 atm. The units in these equations are W, K, m, s, and atm.

Heat is removed from the heated surface during boiling by several simultaneous mechanisms:

1 As latent heat content of bubbles, $(q/A)_e$
2 By convection caused by bubble agitation of the boundary layer, $(q/A)_a$
3 By condensation at the top of the growing bubble while still attached to the wall
4 By single phase heat transfer between patches of bubbles, $(q/A)_{sp}$

The first three mechanisms are discussed by Forster and Greif (1958) who showed that the second, i.e., $(q/A)_a$, was sufficient to account for the high heat transfer at atmospheric pressure without introducing the third. The evaporative heat flux, $(q/A)_e$, is small at atmospheric pressure, but increases with pressure.

Neglecting the third mechanism, we may write

$$\frac{q}{A} = \left(\frac{q}{A}\right)_e + \left(\frac{q}{A}\right)_a + \left(\frac{q}{A}\right)_{sp} \tag{5}$$

It may be shown readily that

$$\left(\frac{q}{A}\right)_e = nfB_d\rho_g\lambda \tag{6}$$

The agitation heat flux, $(q/A)_a$, arises in the following manner. As a bubble grows, it pushes superheated liquid in front of it into the subcooled bulk fluid. When it detaches from the heated surface, it continues to push hot liquid away from the wall in the drift flow, while colder liquid from the bulk rushes to the wall. Thus, a quantity of cold water related to the bubble volume is drawn to the heated surface, heated through an effective temperature difference, τ, and pushed out again by the bubble. Thus, we may write

$$\left(\frac{q}{A}\right)_a = nfB_d\rho_l C_p \tau \tag{7}$$

where τ is related to the bulk temperature, the degree of superheat at the wall, and the efficiency with which the bubble circulates the water. Therefore, Bowring has to introduce a second empirical parameter, π, defined as

$$\pi = \frac{(q/A)_a}{(q/A)_e} = \frac{\rho_l C_p}{\rho_g \lambda} \tag{8}$$

whose value must be obtained from experimental data.

Bowring further assumes that the heat flux in subcooled boiling at a given surface temperature is independent of subcooling and velocity, if boiling is "fully developed." Finally, Bowring assumes, as already mentioned, that the heat exchange caused by bubble recondensation is negligible. This consequently means that bubble collapse is so small that it has no influence on the void. This certainly is true only in the slightly subcooled region.

Using the mass balance equations for both the subcooled and the bulk boiling region, Bowring gets the following relationship between void fraction and mass fraction quality:

$$\frac{\alpha}{1-\alpha} = \frac{X}{S}\frac{\rho_l}{\rho_g}(1-X) \tag{9}$$

In the bulk boiling region, all the heat transfer eventually is converted to latent heat of vaporization, so that the steam quality can be written as

$$X = \left(\frac{P_h}{\rho_l} Av\lambda\right)\int_{ML}^{z}\left(\frac{q}{A}\right)dz \qquad z > z^* \tag{10}$$

In the slightly subcooled region only the evaporative component of the heat flux, $(q/A)_e$, is used to produce steam, the rest going to raise the bulk temperature. The equation describing the rise of steam quality analogous with the bulk boiling equation may be written as

$$X_b = \left(\frac{P_h}{\rho_l} Av\lambda\right)\int_{z_r}^{z}\left(\frac{q}{A}\right)dz \tag{11}$$

Substituting from Eqs. (5) and (8), where θ_{sp} is given by

$$\left(\frac{q}{A}\right)_{sp} = h\theta \qquad \theta > \theta_{sp} \tag{12}$$

where

$$\theta_{sp} = \frac{0.7q}{Ah} - \beta\left(\frac{0.7q}{A}\right)^{0.25} \tag{13}$$

In terms of void fraction one finally gets

$$\frac{\alpha_b(1 - X_b)}{1 - \alpha_b} = \frac{P_h}{\rho_g A v \lambda S}\int_{z_r}^{z} \frac{(q/A) - (q/A)_{sp}}{1 + \pi}\,dz \tag{14}$$

or, integrated

$$\frac{\alpha_b(1 - X_b)}{1 - \alpha_b} = \frac{P_h}{\rho_g A v \lambda S(1 + \pi)}\left(\frac{\bar{q}}{A}\right)_{scb}(z - z_r) \tag{15}$$

In this equation, z_r is the point in the channel where θ_r is reached, which can be easily calculated if the longitudinal heat-flux distribution is known and if no mixing is assumed. The weight fraction, X_b, may be calculated from

$$X_b = \frac{P_h}{\rho_l A v \lambda(1 + \pi)}\left(\frac{\bar{q}}{A}\right)_{scb}(z - z_r) \tag{16}$$

In most cases X_b is small and may be neglected.

4.2 Theory Given by Rouhani

A detailed literature survey on the papers dealing with the calculation of void fraction in subcooled boiling was given by Rouhani (1968). Several additional reports on this subject have appeared in the literature. Among these are the works of Levy (1966) and Zuber (1966). The main point of the paper by Levy is a new method of calculating the liquid subcooling at the point of the bubble departure. This is different from Bowring's method. Levy suggests also a certain relationship between the true local vapor void fraction and the corresponding thermal equilibrium value. Finally, by applying an accepted slip correlation, he calculates the void fraction in subcooled boiling.

Rouhani considers two regions of subcooled boiling:

1 Local boiling with bubbles not detaching from the heated surface and high subcooling
2 Local boiling with bubble detachment and flow of vapor bubbles with liquid

He assumes that the maximum value of wall voidage, α_c, occurs at the end of the first region. He calculates the voidage at this point by the simple equation

$$\alpha_c = 2.435 \times 10^{-3} p^{-0.237} \frac{P_h}{A_c} \tag{17}$$

This equation is not written in a dimensionless form and, therefore, the pressure p is to be given in N/m^2 and it is valid only for water as the boiling medium. P_h is the perimeter and A_c is the flow area in the channel with the dimensions m and m^2, respectively.

Rouhani assumes that local boiling starts at a point where

$$\frac{q}{A} - h(t_s - t_l) > 0 \tag{18}$$

In this equation, h is the single-phase heat-transfer coefficient for only liquid flow, which can be calculated by using Collburn's correlation

$$h = \frac{0.023}{\text{Re}^{0.8}} G C_p \text{Pr}^{0.8} \tag{19}$$

At high subcooling, the single-phase heat transfer will be still effective but accompanied by the other mechanisms. With decreasing subcooling, the heated surface will become more and more covered with bubbles and hence less accessible to the bulk liquid flow. For this reason, Rouhani assumes that the nonboiling fraction of the heat flux will be

$$\left(\frac{q}{A}\right)_{\text{nb}} = \left(1 - \frac{\alpha}{\alpha_c}\right) h(t_s - t_l) \qquad \alpha > \alpha_c \tag{20}$$

in which α is the local void fraction and α_c is the void fraction at the point of vapor clotting.

The total heat balance on the heated surface is

$$\frac{q}{A} = h\theta_l \left(1 - \frac{\alpha}{\alpha_c}\right) + \dot{m}_s \lambda + \frac{\dot{m}_s}{\rho_g} C_p \rho_l \theta_l \tag{21}$$

The amount of the heat that goes to the steam generation can be easily calculated by a simple energy balance.

$$dQ_b = \dot{m}_s \lambda P_h \, dz = \frac{(q/A) - h\theta_l(1 - \alpha/\alpha_c)}{\rho_g \lambda + C_p \rho_l \theta_l} \tag{22}$$

Finally, the amount of heat that goes to the subcooled liquid through condensation of vapor bubbles can be expressed as

$$dQ_c = k_c \theta_l \, dz \tag{23}$$

where k_c is a condensation coefficient with the same dimensions as that of the thermal conductivity. Rouhani shows that this constant is actually proportional to the thermal conductivity of the liquid phase divided by the Prandtl number.

Considering the heat balance in the axial direction, one can use two separate equations for each of the two phases. Both phases are connected by Eq. (23), which gives the heat transferred from the vapor to the liquid.

For the vapor, one can generally write the heat balance as

$$dX = \frac{dQ_b - dQ_c}{\dot{m}\lambda} \tag{24}$$

This is the differential change in the true vapor fraction with dz regardless of the flow regime or slip ratio.

The total heat balance across dz gives the differential change in the true liquid subcooling as

$$d\theta_l = \frac{(q/A)P_h \, dz - (dQ_b - dQ_c)}{\dot{m}C_p(1 - X)} \tag{25}$$

Now, assuming that the variations of dQ_b and dQ_c with z are known, one may integrate Eq. (24) to obtain the true steam quality at any height. In addition, one has to use a suitable relationship for slip ratio and can calculate the local values of the void volume fraction.

For the relationship between the local void and the mass flow rate quality, that is, for indirectly expressing the slip ratio, Rouhani used a derivation given by Zuber and Findlay (1965), which has the form

$$\alpha = \frac{X}{\rho_g}\left\{C\left(\frac{X}{\rho_g} + \frac{1-X}{\rho_l}\right) + \frac{1.18}{G}\left[\frac{\sigma g(\rho_l - \rho_g)}{\rho_l^2}\right]^{0.25}\right\}^{-1} \tag{26}$$

In this equation, C is a distribution parameter, which is dependent on the velocity profile and void distribution over the flow area. Rouhani found that, over a wide field of parameters, an average value of about 1.1 for this distribution parameter C is adequate, and only at lower mass velocities a strong dependence of C on this parameter is given, and in this region the value may be much larger than 1.1.

The condensation coefficient k_c is dependent on many parameters, for example, on the thermal conductivity of the liquid, on the local values of contact area between vapor and liquid, which depends on the void fraction, on channel geometry, on mass velocity, and on heat-flux density. In a systematic analysis comparing experimental data with analytical deliberations, Rouhani found the following correlation for the condensation coefficient k_c.

$$k_c = \alpha \frac{k_l}{\mathrm{Pr}} \left(\frac{\rho_g}{\rho_l}\right)^2 A_c^{213} \alpha^{213} \frac{\mathrm{Re}_l}{N_q^{0.5}} \tag{27}$$

In this equation, k_l is the thermal conductivity of the liquid, Pr the Prandtl number, Re the Reynolds number and N_q a dimensionless number taking in account the effect of heat flux on the heat transport between vapor and liquid, as given in Eq. (28).

$$N_q = \frac{(q/A)\mu_l}{\lambda(\rho_l - \rho_v)} \tag{28}$$

Finally, in Eq. (28), a is a dimensional constant, which probably may depend on the number of nucleation sites per unit area of the heated surface and on the bubbling frequency, which has a value of 30 $\mathrm{m}^{-4/3}$.

Thus, by numerical integration of Eqs. (22)-(25) and using Eqs. (26)-(28), one can calculate the local void fraction with subcooled boiling.

Rouhani made a very detailed comparison of his theoretical results with experimental data. In Fig. 14, an example for such a comparison is given. This example shows that there is an excellent agreement between measurements and theory. Only at very low mass velocities, i.e., below 130 kg/m^2-s, the theory gives a void, which is about 20 percent higher than the measurements. This may be caused by an effect of mass velocity on the rate of condensation or on the effect of variations of physical properties because of the large temperature variations. There certainly also may arise an intensified convec-

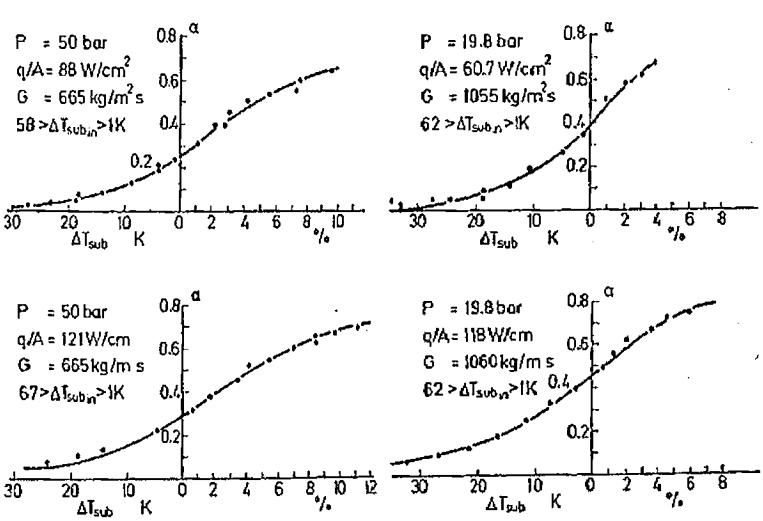

FIG. 14 Comparison of calculated data with data of Rouhani (1966).

tion at very low mass velocities, and a heat removal by such mechanisms has not been accounted for in the calculations.

Generally one can say that, based on the results of comparison, the model of Rouhani gives a very close approximation of the physical phenomena involved in the changes of void fraction in flow boiling throughout the boiling regions.

NOMENCLATURE

a	a dimensional constant (m^{-413})
a_1	a dimensional constant (m^{-413})
a_2	a proportionality constant
A_b	contact area between the bubbles and the liquid per unit length of the channel (m^2)
A_c	flow area in the channel (m^2)
B_d	bubble volume (m^3)
C	distribution parameter
C_p	specific heat of liquid at constant pressure (J/kg-°C)
D_e	equivalent hydraulic diameter, $4A_c/P_t$ (m)
f	bubble repetition rate while growing on the wall (s^{-1})
G	mass velocity (kg/m^2-s)
h	heat transfer coefficient (Collburn's correlation) (W/m^2-°C)
i	inlet
k_c	condensation factor (W/m-°C)
k_l	thermal conductivity of liquid (W/m-°C)
L	length of heated channel (m)
M	fractional length of channel before bulk boiling would start if there were no subcooled void
$\dot{m}$	total mass flow rate (kg/s)
$\dot{m}_s$	mass of liquid which is converted into steam per unit time per unit area of the heated surface (kg/m^2-s)
N_q	a dimensionless number
n	number of bubble sites per unit area of heated surface (m^{-2})
p	pressure (N/m^2)
P_h	heated perimeter (m)
Pr	Prandtl number: $C_p \rho_1 / k_l$
q/A	heat flux (W/m^2)
Q_b	the amount of heat absorbed by boiling per unit time per unit length of channel (W/m)
Q_c	the amount of heat exchanged by condensation of bubbles per unit time per unit length of channel (W/m)
Re	Reynolds number: $G(D_e/\mu)$
S	slip ratio: v_g/v_l
t_l	liquid temperature in the presence of steam flow (°C)

t_s saturation temperature (°C)
t_w wall temperature (°C)
v liquid velocity at channel inlet (m/s)
X true vapor weight fraction (steam quality)
X_0 average steam quality
z distance along the heated channel measured from the inlet (m)
α vapor volume fraction (void)
α_c upper limit of wall voidage 7.8 exp $[-0.0163(p-1)]$
θ_d subcooling at bubble detachment (°C)
ϵ a pressure-dependent nondimensional parameter
η_l subcooled void parameter; value given by Eq. (4)
θ_l liquid subcooling as an integral of Eq. (25), $t_s - t_l$ (°C)
θ_d subcooling at bubble formation
θ_0 average liquid subcooling obtained from a heat balance for the whole flow (°C)
λ latent heat of vaporization (J/kg)
μ_l dynamic viscosity of liquid (kg/ms)
π subcooled void parameter; value given by Eq. (8)
ρ_g vapor density (kg/m^3)
ρ_l liquid density (kg/m^3)
σ surface tension of liquid (N/m)
τ $\pi(\rho_g\lambda)/(\rho_l C_p)$

Subscripts

a agitation
b bubble
d at bubble detachment
e "evaporative"
M at $z = ML$
r at the point of rapid rise in subcooled void fraction saturation subcooled
s saturation
scb subcooled boiling
sp single phase
w wall
$-$ average value
$*$ at intersection of subcooled and bulk boiling void curves

REFERENCES

Beer, H. (1969). *Progr. in Heat and Mass Transfer*, vol. 2, pp. 311–370.
Bowring, R. W. (1962). Physical Model, Based on Bubble Detachment and Calculations of Steam Voidage in Subcooled Region of a Heated Channel, *HPR* 10.
Forster, K. E., and Greif, R. (1958). *Paper* 58, *AIChE Heat Transfer Conf.*, Chicago.
Forster, H. K., and Zuber, N. (1955). *AIChE J.*, vol. 1, no. 4, pp. 531–535.

Han, Ch. Y., and Griffith, P. (1965). *Int. J. Heat Mass Transfer*, vol. 8, pp. 887–914.

Jens, W. H., and Lottes, P. A. (1951). *ANL*-4627.

Lavigne, P. (1962). Rapport *GEA* no. 2365.

Levy, S. (1966). Forced Convection Subcooled Boiling-Prediction of Vapor Volumetric Fraction, *GEAP*-5157.

McAckunas, F. A., and Winter, E. R. F. (1971). *Int. Symp. Two Phase Systems*, Haifa, Israel, Pap. No. 1-15.

Plesset, M. S., and Zwick, S. A. (1954). *J. Appl. Phys.*, vol. 25, no. 4, pp. 493–500.

Rouhani, S. Z. (1966). Void Measurements in the Region of Subcooled and Low Quality Boiling, pt. 2, *AE*-239.

Rouhani, S. Z. (1968). Calculation of Steam Volume Fraction in Subcooled Boiling, *J. Heat Transfer*, vol. 90, pp. 158–164.

Rouhani, S. Z., and Axelsson, E. (1970). Calculation of Void Volume Fraction in the Subcooled and Quality Boiling Regions, *Int. J. Heat Mass Transfer*, vol. 13, pp. 383–393.

Tong, L. S. (1967). Boiling Heat Transfer and Two-Phase Flow, John Wiley & Sons, Inc., New York.

Zuber, N., and Findlay, J. (1965). Average Volumetric Concentration in Two-Phase Flow Systems, *J. Heat Transfer*, vol. 87, ser. C, pp. 453–462.

Zuber, N., Staub, F. W., and Bijwaard, G. (1966). Vapor Void Fraction in Subcooled Boiling and in Saturated Boiling Systems, *3rd Int. Heat-Transfer Conf.*, *ASME*-153.